

Spatial Representation of Temporal Information by Networks that Learn

Thomas Nowotny* and Misha I. Rabinovich†

Institute for Nonlinear Science, University of California San Diego, 9500 Gilman Drive, La Jolla, CA 92093-0402

Henry D. I. Abarbanel‡

*Institute for Nonlinear Science, Department of Physics
and*

*Marine Physical Laboratory (Scripps Institution of Oceanography),
University of California, San Diego,
La Jolla, CA 92093-0402*

In networks that learn the coupling strengths among neurons are altered according to some rule which is implemented as input signals are presented to the network. We investigate here a mechanism, based on the observed response of biological synapses to presynaptic and postsynaptic spikes at excitatory synapses, for storing, retrieving and predicting temporal sequences. Our model system is composed of realistic conduction based Hodgkin-Huxley neurons operating in a spiking mode and densely coupled with learning synapses. After conditioning through repeated input of a limited number of temporal sequences the system is able to predict the temporal sequences upon receiving a new input comprised of a fraction of the original training sequence. This is an example of effective unsupervised learning. We investigate the dependence of learning success on entrainment time, system size and the presence of noise. There are implications from this modeling for learning of motor sequences, recognition and prediction of temporal sensory information in the visual as well as auditory systems and for late processing in the olfactory system.

I. INTRODUCTION

Animals are challenged in various ways to learn, produce, reproduce and predict temporal patterns. A prominent example are the numerous motor programs necessary to interact efficiently with the environment. One specific manifestation is the vocal motor system of song birds. It has been shown that the temporal sequence of syllables in a bird's song corresponds to temporal sequences of bursts in the neurons of the forebrain control system [1, 2]. These are learned and stored by the adolescent bird.

Temporal codes seem to be used for a variety of other tasks as well. Temporal coding in the retina [3] is an example, as is information transport in the olfactory system of the locust. In the latter it has been shown that the purely identity coded information of the receptor neurons is transformed into an identity-temporal code inside the antennal lobe [4, 5, 6].

It is an open question how the learning and memory of time sequences is accomplished in real neural systems. Three main principles for representing time in neural systems are frequently discussed:

- The first makes use of delays and filters. There are various ways of processing of temporal information in the dendritic tree [7, 8, 9, 10] or through axonal delays [11, 12, 13, 14]. Other examples are mul-

tilayer neural networks in which the delay of the synaptic connections between layers allows to represent or decode temporal information and propagating waves as known from the thalamo-cortical system [15, 16].

- The second principle rests on feedback. Through delayed feedback temporal information can be processed on the level of individual neurons as well as on the level of larger structures. A prominent example for this are recurrent multi layer neural networks which play a role in sequence memory in the hippocampus [17, 18].
- The third principle is to transform the temporal information into spatial information. This can occur through the dynamics of a network with asymmetric lateral inhibition [19]. In this paper we demonstrate an alternative mechanism which maps the temporal information to the strength of synapses in a network through spike timing dependent plasticity (synaptic plasticity). Similar mechanisms have been suggested for predictive activity and direction selectivity in the visual system [20] and learning in the hippocampus [17, 18, 21] as well as prediction in hippocampal place fields and route learning in rats [22, 23, 24]. In contrast to these earlier works we use realistic conductance based model neurons and focus on questions of learning of several distinct input sequences in one system. This learning capability is necessary in order to process the identity-temporal code believed to be generated by winnerless competition in sensory systems [6, 25].

*Electronic address: tnowotny@ucsd.edu; URL: <http://inls.ucsd.edu/~nowotny>

†Electronic address: mrabinovich@ucsd.edu

‡Electronic address: hdia@jacobi.ucsd.edu

Synaptic plasticity in the connections among neurons allows networks to alter the details of their interaction

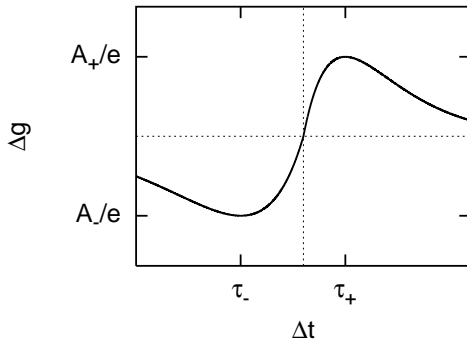


FIG. 1: Synaptic plasticity learning rule. $\Delta g = A_+ \frac{\Delta t}{\tau_+} e^{-\Delta t/\tau_+}$ for $\Delta t > 0$ and $\Delta g = A_- \frac{\Delta t}{\tau_-} e^{\Delta t/\tau_-}$ for $\Delta t < 0$, $A_+, A_- > 0$.

and develop memories of previous input signals. The details of the methods by which biological neurons express plasticity at synapses is not fully understood at the biophysical level, but many aspects of the phenomena which occur when presynaptic and postsynaptic neurons are jointly activated are now becoming clear. First of all, it seems well established that activity at both the presynaptic and the postsynaptic parts of a neural junction is required for the synaptic strength to change. Arrival of a presynaptic action potential will induce, through normal neurotransmitter release and reception by postsynaptic receptors, a postsynaptic electrical action which generally leads to no change in the coupling strength at that synapse. Depolarization of the postsynaptic cell by various means *coupled with* arrival of a presynaptic action potential can lead to changes in synaptic strength in a variety of experimental protocols. It is quite important that changes in the synaptic strength, which we denote in terms of a conductivity change Δg can be either positive, called potentiation, or negative, called depression. When the expression of Δg is long lasting, several hours or even much longer after induction, increases in g are called long term potentiation or LTP, and decreases in g are called long term depression or LTD. Good reviews of the current situation are found in [26, 27, 28].

LTP and LTD can be induced by (1) depolarizing the postsynaptic cell to a fixed membrane voltage and presenting presynaptic spiking activity at various frequencies, by (2) inducing slow (LTD) or rapid (LTP) release of Ca^{2+} [29], or by (3) activating the presynaptic terminal a few tens of milliseconds before activating the postsynaptic cell, leading to LTP, or presenting the activation in the other order, leading to LTD [30, 31].

In this paper we study numerically a network composed of realistic Hodgkin-Huxley (HH) conductance based spiking model neurons which are densely coupled with synaptic interactions whose maximal conductances are permitted to change in accordance with the observations on closely spaced spike arrival times to the presynaptic and postsynaptic junctions of the synapse.

The response of a learning synapse to the arrival of a presynaptic spike at t_{pre} and a postsynaptic spike at t_{post} is a function only of $\Delta t = t_{\text{post}} - t_{\text{pre}}$ and for $\Delta t > 0$ $\Delta g(\Delta t)$ is positive, LTP, and for $\Delta t < 0$ $\Delta g(\Delta t)$ is negative, LTD.

$$\begin{aligned} \Delta g(\Delta t) &= A_+ \frac{\Delta t}{\tau_+} e^{-\frac{\Delta t}{\tau_+}} \quad \text{for } \Delta t > 0 \\ \Delta g(\Delta t) &= A_- \frac{\Delta t}{\tau_-} e^{\frac{\Delta t}{\tau_-}} \quad \text{for } \Delta t < 0 \end{aligned} \quad (1)$$

where A_+ , A_- , τ_+ and τ_- are positive constants (see Fig. 1). For many mammalian *in vitro* or cultured preparations the characteristic LTD time τ_- is about two or three times longer than the characteristic LTP time τ_+ . This leads to a preference for LTP at higher frequency stimulation of synaptic plasticity [32].

Here we inquire how a network composed of familiar ion channel conductance based neurons can develop preferred spatial patterns of connectivity when interacting through synapses which update their strength according to the rule just given. This rule is a simplification, which applies for our setting of spiking neurons, of a more general framework [32] which indicates how $\Delta g(\Delta t)$ behaves under stimulus of arbitrary presynaptic and postsynaptic waveforms.

The transformation of temporal information into synapse strength through synaptic plasticity maps a temporal sequence of excitations of neurons to a chain of stronger or weaker synapses among these neurons. If the synapses are excitatory, a strengthened chain of synapses facilitates subsequent excitations of the same temporal pattern up to a point that activation of a few neurons from the temporal sequence allows the system to complete the remaining sequence. The temporal sequence thus have been learned by the system. We demonstrate this type of sequence learning in a computer simulation of a system with realistic model neurons and investigate the reliability of learning, the storage capacity in terms of the number of stored sequences, the scaling of both with system size and the robustness against different types of noise.

II. MODEL SYSTEM

A. Components and Connections

To explore the learning principle for realistic model neurons we simulated a network with the topology shown in Fig. 2. In this network n HH conductance based model neurons are connected all-to-all while each neuron also receives input from one “input neuron” (filled ovals in Fig. 2).

The HH model we use is composed of four ion channels and a leak current supplemented by a synaptic input. We have for the membrane voltage of any component of the

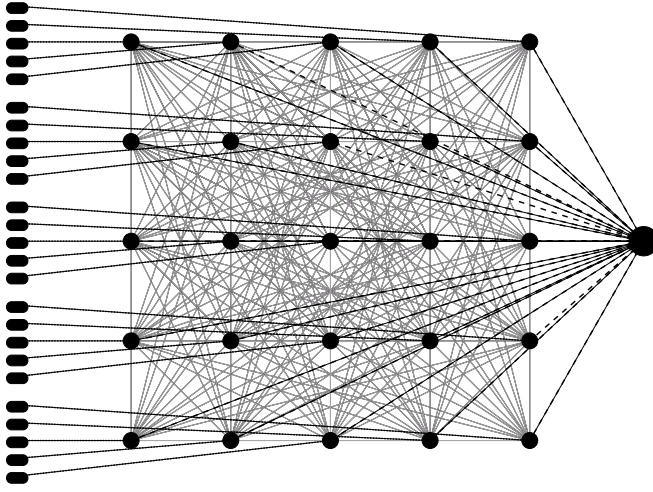


FIG. 2: Morphology of the model system. The ovals are artificial input neurons producing rectangular spikes of 3 ms duration at specified times. Each is connected by a non-plastic excitatory synapse to one of the neurons in the main ‘‘cortex’’ (dotted lines). The full circles depict the Hodgkin-Huxley type neurons of the main ‘‘cortex’’. They are connected all-to-all by plastic synapses shown as solid gray lines. The big full circle on the right depicts a neuron with slow Calcium dynamics which inhibits all neurons in the ‘‘cortex’’ through the non-plastic synapses shown as dashed lines.

network

$$C \frac{dV(t)}{dt} = - (I_{\text{Na}}(t) + I_{\text{K}}(t) + I_{\text{Ca}}(t) + I_{\text{KCa}}(t) + I_{\text{Leak}}(t)) + I_{\text{Synapse}}(t), \quad (2)$$

where $V(t)$ is the membrane voltage, $C = 1.0 \mu\text{F}$ is the membrane capacitance, and the ion currents are determined by

$$\begin{aligned} I_{\text{Na}}(t) &= m(t)^3 h(t) g_{\text{Na}}(V(t) - V_{\text{Na}}) \\ I_{\text{K}}(t) &= n(t)^4 (V(t) - V_{\text{K}}) \\ I_{\text{Ca}}(t) &= k(t)^3 l(t) g_{\text{Ca}} \frac{V(t)}{1 - e^{2V(t)/k_{\text{Ca}}}} \\ I_{\text{KCa}}(t) &= g_{\text{KCa}}(V(t) - V_{\text{KCa}}) \frac{\omega(t)^4}{k_{\text{KCa}}^4 + \omega(t)^4}, \end{aligned} \quad (3)$$

and the leak current is

$$I_{\text{Leak}}(t) = g_{\text{Leak}}(V(t) - V_{\text{Leak}}). \quad (4)$$

We used the following values for the maximal conductances and reversal potentials: $g_{\text{Leak}} = 0.1 \text{ mS}$, $g_{\text{Na}} = 50 \text{ mS}$, $g_{\text{K}} = 10 \text{ mS}$, $g_{\text{Ca}} = 0.2 \text{ mS}$, $g_{\text{KCa}} = 0.15 \text{ mS}$, $V_{\text{Leak}} = -55 \text{ mV}$, $V_{\text{Na}} = 50 \text{ mV}$, $V_{\text{K}} = -95 \text{ mV}$, $V_{\text{KCa}} = -95 \text{ mV}$, and the constants are $k_{\text{KCa}} = 0.15$ and $k_{\text{Ca}} = 24.42 \text{ mV}$.

Each of the activation and inactivation functions $m(t)$, $h(t)$, $n(t)$, $k(t)$, and $l(t)$ satisfy a first order kinetics equation of the form

$$\frac{dX(t)}{dt} = A_X(V(t)) - B_X(V(t))X(t), \quad (5)$$

where for $X(t) = m(t)$, $h(t)$, and $n(t)$

$$\begin{aligned} A_X(V) &= \alpha_X(V) \\ B_X(V) &= \alpha_X(V) + \beta_X(V) \\ \alpha_m(V) &= 0.116 \frac{V + 42 \text{ mV}}{1 - \exp(-(V + 42 \text{ mV})/4 \text{ mV})} \\ \beta_m(V) &= -0.093 \frac{V + 15 \text{ mV}}{1 - \exp((V + 15 \text{ mV})/5 \text{ mV})} \\ \alpha_h(V) &= 0.0426 \exp(-(V + 38 \text{ mV})/18 \text{ mV}) \\ \beta_h(V) &= \frac{1.33}{1 + \exp(-(V + 15 \text{ mV})/5 \text{ mV})} \\ \alpha_n(V) &= 0.01 \frac{V + 30 \text{ mV}}{1 - \exp(-(V + 30 \text{ mV})/5 \text{ mV})} \\ \beta_n(V) &= 0.166 \exp(-(V + 35 \text{ mV})/40 \text{ mV}). \end{aligned} \quad (6)$$

For $k(t)$ and $l(t)$ we have

$$\begin{aligned} A_X(V) &= \frac{\alpha_X(V)}{\beta_X(V)} \\ B_X(V) &= \frac{1}{\beta_X(V)} \\ \alpha_k(V) &= \frac{1}{1 + \exp(-(V + 27.1 \text{ mV})/7.18 \text{ mV})} \\ \beta_k(V) &= 20 - \frac{19.9}{1 + \exp((V - 40.1)/8 \text{ mV})} \\ \alpha_l(V) &= \frac{1}{1 + \exp((V + 27.0 \text{ mV})/3.5 \text{ mV})} \\ \beta_l(V) &= 30 + \frac{100}{1 + \exp((V + 50.1 \text{ mV})/5 \text{ mV})}. \end{aligned} \quad (7)$$

The Ca induced K current activation is governed by $\omega(t)$ satisfying

$$\frac{d\omega(t)}{dt} = 0.001 \left(-\frac{I_{\text{Ca}}(t)}{\mu\text{A}} - c_0^2 \omega(t) + 0.04 c_0^2 \right), \quad (8)$$

and $c_0 = 1.8$. The typical response of this type of neuron to input current pulses is depicted in Fig. 3. The typical dynamics of the neurons in the model network is shown in the first five rows of Fig. 4.

The ‘‘input neurons’’ generate rectangular spikes of 3 ms duration at times determined by externally chosen input sequences. Each of these spikes is sufficient to trigger exactly one spike in the receiving neuron (see Fig. 3). The input sequences are chosen such that only one ‘‘input neuron’’ spikes at any given time and the time between input spikes was fixed to 10 ms.

A neuron connected to all neurons in the network (large filled circle in Fig. 2) provides global inhibition whenever the activity in the network exceeds a certain threshold. The inhibitory neuron has only a slow Calcium dynamics and is modeled by

$$\frac{dV_I(t)}{dt} = -\frac{1}{C} (I_l(t) + I_{\text{Ca}}(t) + I_{\text{KCa}}(t) - I_{\text{Synapse}}), \quad (9)$$

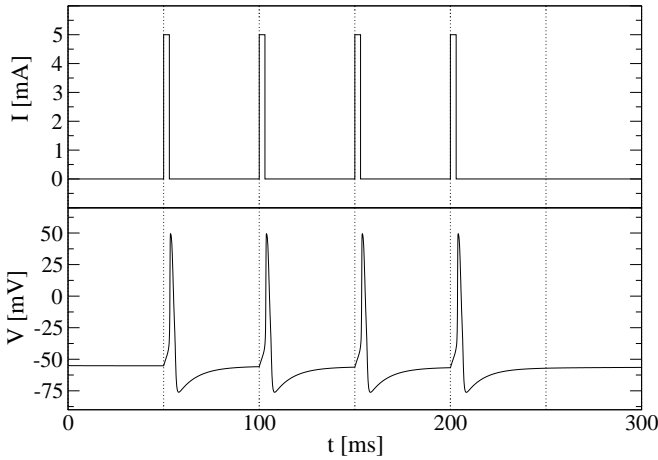


FIG. 3: Typical response of the HH type model neurons to input current pulses. The neuron responds with isolated spikes in the parameter regime used in this work.

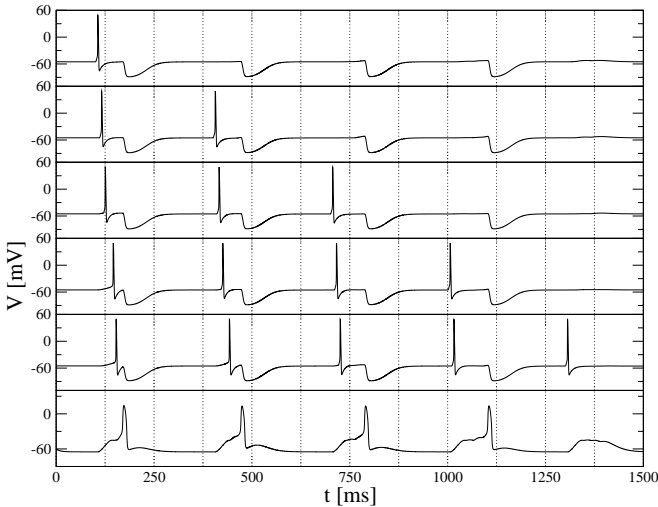


FIG. 4: Typical dynamics of the HH type model neurons in the network (recalling stage). Rows one through five show the activity of five neurons belonging to one of the memorized sequences. The last row shows the membrane potential of the globally inhibitory neuron.

where

$$\begin{aligned}
 I_l(t) &= g_l(V(t) + 65 \text{ mV}) \\
 I_{\text{Ca}}(t) &= g_{\text{Ca}} k(t)^3 l(t) \frac{V(t)}{1 - \exp(2V(t)/k_{\text{Ca}})} \\
 I_{\text{KCa}}(t) &= g_{\text{KCa}} \frac{\omega(t)^4}{\omega(t)^4 + 0.5^4} (V(t) + 70 \text{ mV}),
 \end{aligned} \quad (10)$$

and $g_l = 0.1 \text{ mS}$, $g_{\text{Ca}} = 2.5 \text{ mS}$, $g_{\text{KCa}} = 2.0 \text{ mS}$, and again $k_{\text{Ca}} \approx 24.42 \text{ mV}$. The typical dynamics of the inhibitor is shown in the last row of Fig. 4.

Our model of the synapses comes from Rall [33, 34] and now is a standard model for simplified synaptic dy-

namics [35]. In particular, we use

$$I_{\text{Synapse}} = -k_{\text{syn}} g(t) (V_{\text{post}}(t) - V_{\text{syn}}), \quad (11)$$

where $g(t)$ satisfies

$$\begin{aligned}
 \frac{df(t)}{dt} &= \frac{1}{\tau_{\text{syn}}} (\Theta(V_{\text{pre}}(t) - V_{\text{th}}) - f(t)) \\
 \frac{dg(t)}{dt} &= \frac{1}{\tau_{\text{syn}}} (f(t) - g(t)),
 \end{aligned} \quad (12)$$

and $V_{\text{syn}} = 0 \text{ mV}$, $V_{\text{th}} = -20 \text{ mV}$, $\tau_{\text{syn}} = 15 \text{ ms}$, $V_{\text{pre}}(t)$ and $V_{\text{post}}(t)$ are the pre- and post-synaptic membrane potentials and k_{syn} is the strength of the synapse. $\Theta(u) = 0, u \leq 0$ and $\Theta(u) = 1, u > 0$ is the usual Heaviside function.

The synaptic strength of the internal synapses is adjusted according to the synaptic plasticity rule shown in Fig. 1 whenever a spike in their presynaptic and post-synaptic neuron occurs. In itself, this rule may lead to “run-away” behavior of the synaptic strengths. While this may be avoided in the dynamical model of synaptic plasticity [32], we need to address this within the simpler model used here. We do so by two approaches: (1) we add a long term, slow decay to the synaptic plasticity which would, all other factors being absent, bring it back to a nominal allowed level a long time after alteration by our rule. This we implement with

$$\frac{dg_{\text{raw}}}{dt} = -\frac{1}{\tau_g} (g_{\text{raw}}(t) - g_{0,\text{raw}}) \quad (13)$$

where $g_{0,\text{raw}}$ is the initial value of the unmodified synapse strength. So after potentiation or depression according to the synaptic plasticity rule, the synaptic strength is allowed to slowly decay back to its original value. The time scale of this exponential decay is set by $\tau_g \approx 22.2 \text{ s}$. (2) g_{raw} is an intermediate variable which is then translated into the synaptic strength g via a sigmoid saturation rule

$$g = g_{\text{max}} \frac{1}{2} (\tanh(g_{\text{slope}}(g_{\text{raw}} - g_{1/2})) + 1), \quad (14)$$

where g_{max} is the largest allowed value for the synaptic conductivity, and $g_{1/2}$ sets the threshold where saturation to this value is implemented. All data shown in this work was obtained with $g_{\text{max}} = 0.085 \text{ mS}$, $g_{1/2} = 1/2 g_{\text{max}}$ and $g_{\text{slope}} = 1/g_{1/2}$. In addition the globally inhibitory neuron tends to curb the tendency of the network to saturate its synaptic strengths.

These features of our model reflect our lack of knowledge of the biophysical factors setting the synaptic strength in the first place and our equivalent lack of knowledge how these factors bound the eventual rise or fall of synaptic strength. Our assumption in using these rules is that the actual mechanisms, while surely more complicated in detail, will provide the same effective bounding feature.

The complete system is realized in C++ using an order 5/6 variable time step Runge-Kutta algorithm [36]. The error goal per time step was 10^{-8} in all simulations.

This model system mimics the situation of a highly connected piece of cortex receiving input from the neural periphery. Our input can be interpreted in two ways. It might be a single strong excitatory post-synaptic potential (EPSP) received from an upstream neuron which is strong enough to trigger a spike. It could also be interpreted as the coincidence of several weaker EPSPs received from various pre-synaptic neurons being sufficient to cause a spike.

B. Operations and Activity

To test the ability of this network to store (learn) and retrieve (remember) temporal-identity patterns it was trained with a set of randomly chosen sequences of inputs. The learning rate A_+ and the time scale of forgetting τ_g in the synaptic plasticity learning rule were chosen such that learning reached a steady state after a learning time of about 80 s. In particular, $A_+ = 0.039 \text{ mS}$, $A_- = 2/3 A_+$, $\tau_+ = 26 \text{ ms}$, $\tau_- = 3/2 \tau_+$ and $\tau_g \approx 22.2 \text{ s}$.

After the training phase the network was presented with pieces of the training patterns. We presented all possible ordered pieces of one to four input spikes and recorded the number and identity of spiking neurons in the network in response to this input. Perfect learning of the patterns would correspond to obtaining a spike from each of the network neurons in a given pattern when presenting a piece of two or three inputs from that pattern to the “input neurons”. Furthermore, all other network neurons should remain inactive if the pattern is reproduced exactly.

As a result of incomplete or ineffective learning two types of errors can occur. (1) Neurons which should be excited within the given pattern do not spike or (2) neurons which are not supposed to spike do so. Due to overlap of input patterns, the learning efficiency is a function of the number of learned patterns as well as the size of the network.

The probability distribution for the number Y_{ijrkn} of *ordered* j -tuples occurring in at least i out of r patterns with k neurons each for a system with a total number of n neurons is given by

$$P(Y_{ijrkn} = l) = \binom{\frac{n!}{(n-j)!}}{l} (p_j^i)^l (1-p_j^i)^{\frac{n!}{(n-j)!}-l} \quad (15)$$

where p_j^i is the probability to have any given *ordered* j -tuple of neurons in i or more of the r patterns. This is given by

$$p_j^i = \sum_{s=i}^r \binom{r}{s} (p_j)^s (1-p_j)^{r-s} \quad (16)$$

in which p_j is the probability to have a given *ordered* j -tuple in a given pattern with k active neurons,

$$p_j = k \frac{(n-j)!}{n!}. \quad (17)$$

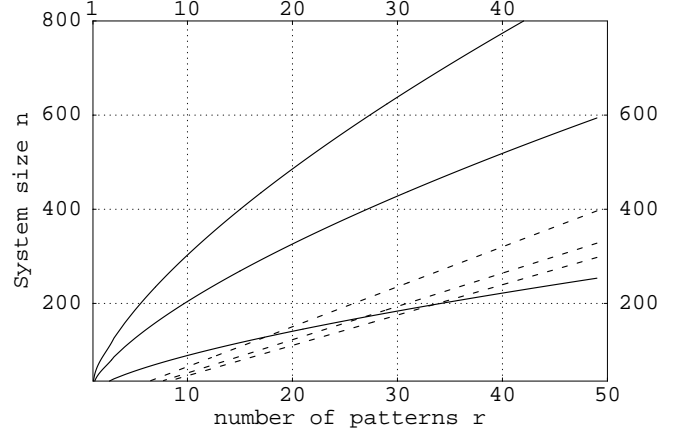


FIG. 5: Estimate for the necessary system size to store a given number of patterns of given length. The dashed lines divide the plane into two regions with $\mathbf{E}Y_{22rkn} < 0.5$ above and $\mathbf{E}Y_{22rkn} > 0.5$ below for $k = 8, 10$, and 12 respectively. The solid lines analogously mark the boundaries between regions with $\mathbf{E}Y_{23rkn} < 0.5$ above and $\mathbf{E}Y_{23rkn} > 0.5$ below.

The probability distribution for the number X_{ijrkn} of *unordered* j -tuples occurring in at least i out of r patterns with k neurons each for a system with a total number of n neurons on the other hand is

$$P(X_{ijrkn} = l) = \binom{\binom{n}{j}}{l} (p_j^i)^l (1-p_j^i)^{\binom{n}{j}-l} \quad (18)$$

where p_j^i is the probability to have any given *unordered* j -tuple of neurons in i or more of the r patterns given by

$$p_j^i = \sum_{s=i}^r \binom{r}{s} (p_j)^s (1-p_j)^{r-s} \quad (19)$$

in which p_j is the probability to have a given *unordered* j -tuple in a given pattern with k active neurons, namely,

$$p_j = \binom{n-j}{k-j} / \binom{n}{k}. \quad (20)$$

The model parameters were chosen such that two to three spikes in a presynaptic neuron are sufficient to excite that neuron. The learning performance is therefore poor as long as there is a significant amount of ordered 2-tuple overlaps in the patterns. The rule of thumb for the expectation value of Y_{ijrkn} , $\mathbf{E}Y_{22rkn} < 0.5$, provides an estimate for the necessary system size n to store r patterns of length k . The dashed lines in Fig. 5 are some examples. An estimate for a sufficient system size is provided by the rule of thumb $\mathbf{E}Y_{23rkn} < 0.5$, i.e. the overlaps in input sequences should have negligible impact on the learning if there is no significant amount of *unordered* 3-tuples occurring in more than one pattern. The resulting estimates are shown as solid lines in Fig. 5

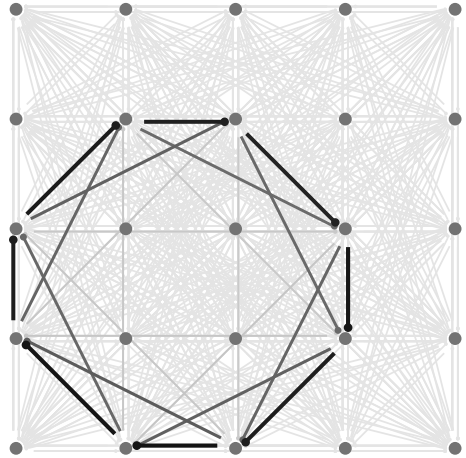


FIG. 6: Simple example of a learned identity-temporal pattern. The neurons at the corners of the octagon have been repeatedly excited in clockwise order. The width and grayscale of the connections encodes the strength of the corresponding synapse and the small circle at the end shows its direction. As one clearly can see the temporal pattern is transformed into an ordered spatial pattern by synaptic plasticity.

III. RESULTS

The synaptic plasticity of synapses transforms time sequences of excitation of neurons into directed spatial patterns as intended. A simple example is shown in Fig. 6 for one input pattern. For randomly chosen input sequences the pattern are structured in the same way but are not so easy to detect with the human eye.

The ability to store more than one pattern was tested with various systems of different size, various numbers and lengths of input patterns and various choices for these input patterns. A typical result for a network of 100 neurons trained with 10 sequences of length 8 is shown in Fig. 7 and 8 and Table I. Fig. 7 shows how the average synaptic strength of synapses between neurons being excited within one of the 10 patterns changes over time during training. Because of the competing effect of the additive learning rule and the implemented exponential decay of synapse strength over time one gets a saturated curve even below the built-in saturation of the synapses.

The response to 3 out of the 8 inputs for each of the 10 input sequences is shown in Fig. 8. The responses to 1 up to 4 inputs averaged over all input sequences are shown in table I. One can clearly see that the learning has more or less already saturated after 80 s of training, compare also the average synaptic strength in Fig. 6.

We took two approaches to test the storage capacity of the system. In one series of simulations a fixed set of 10 input sequences of length 8 was trained by systems of varying size. The learning was tested in the usual way. Fig. 9 shows the results for input sequence fractions of length 2 and 3.

In another series of simulations a network of 50 neu-

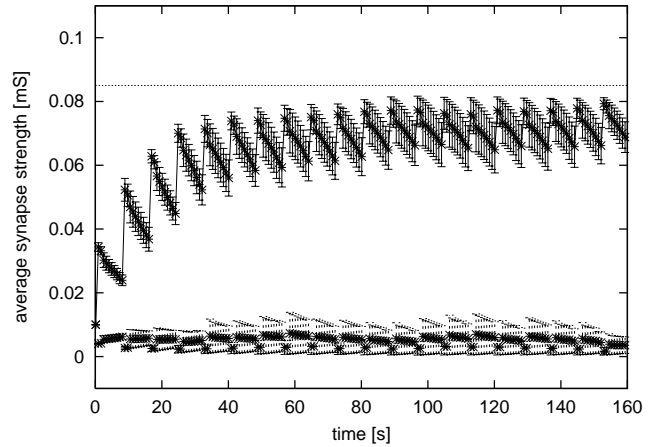


FIG. 7: Development of synaptic strength during training. The network of 100 neurons was trained with 10 patterns of length 8 in sequential order. Each pattern was presented for 0.8 s at a time. The upper line is the average strength of synapses between neurons within one of the trained sequences which point in the direction of the time order in which the neurons appear in the sequence. The lower line is the average strength of the synapses between these neurons in reverse direction. The sharp rises in synaptic strength correspond to training of the particular sequence shown here and the falling flanks correspond to the decay while other patterns are trained.

t [s]	inputs			
	1	2	3	4
80 (in)	1.0 ± 0.0	3.41 ± 1.84	5.09 ± 1.64	5.9 ± 1.27
80 (out)	0.0 ± 0.0	0.09 ± 0.58	0.46 ± 1.08	0.8 ± 1.45
160 (in)	1.0 ± 0.0	3.41 ± 1.77	5.38 ± 1.66	5.98 ± 1.36
160 (out)	0.0 ± 0.0	0.91 ± 1.96	1.26 ± 1.76	1.23 ± 1.42

TABLE I: Response (number of spiking neurons) to one up to four inputs after 80 s and 160 s of training of a system of 100 neurons with 10 randomly chosen input sequences of 8 neurons each. Multiple excitation of one neuron during an input sequence was excluded. (in = neurons spiking belonging to the presented sequence, out = neurons spiking but not belonging to the sequence)

rons was trained with 2 up to 10 sequences of length 8. For each number of sequences ten independent sets of randomly chosen sequences were tested. Fig. 10 shows the average response of the trained systems to 2 and 3 inputs taken from the learned sequences. Averages are over all possible subsequences and all 10 input sequence sets for each data point.

IV. ROBUSTNESS

Biological neural systems are subject to various external and internal noise sources. Starting from internal

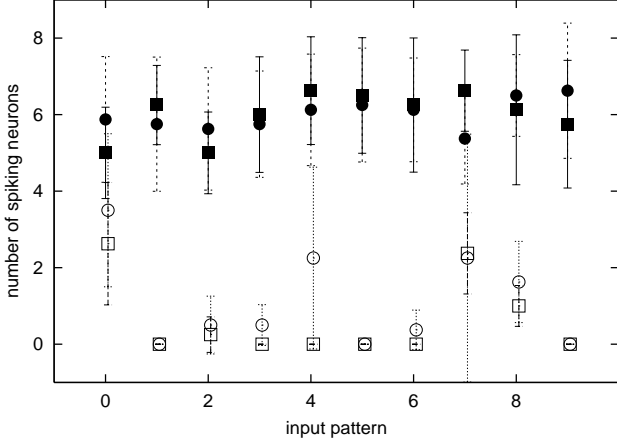


FIG. 8: Learning success for a 100 neuron network after 80 s and 160 s of sequential training with 10 input sequences of length 8. The filled squares show the average number of spiking neurons within a sequence and the open squares the number of spiking neurons not in the sequence in response to the input of fractions of length three from the trained sequences after 80 s of training. The filled circles and the open circles show the corresponding average responses after 160 s of training.

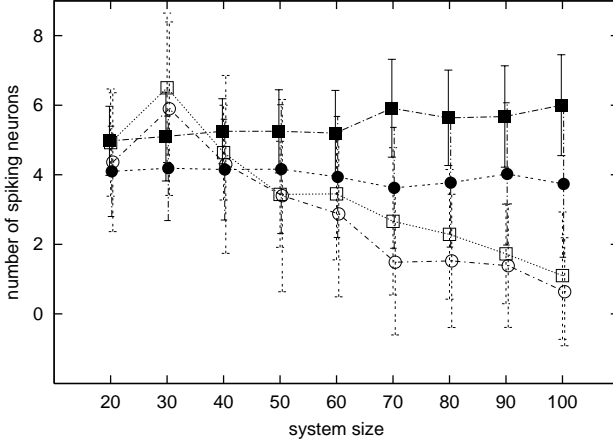


FIG. 9: Scaling of storage capacity with system size. Systems of varying size have been trained with 10 input sequences of length 8 for a total time of 16 s each. The filled squares show the number of spiking neurons within an input sequence in response to inputs of length 3 from that sequence. The open squares show the number of responding neurons not in the sequence. The filled circles and the open circles show the corresponding numbers in response to inputs of length 2.

thermal noise within the system this ranges over noisy or unreliable input and influences from other parts of the organism up to external electromagnetic fields. To test the effect of noise on the learning success of our model systems we focused on two types of noise. We implemented a Gaussian white noise in the Hodgkin-Huxley type model neurons and we implemented unreliable in-

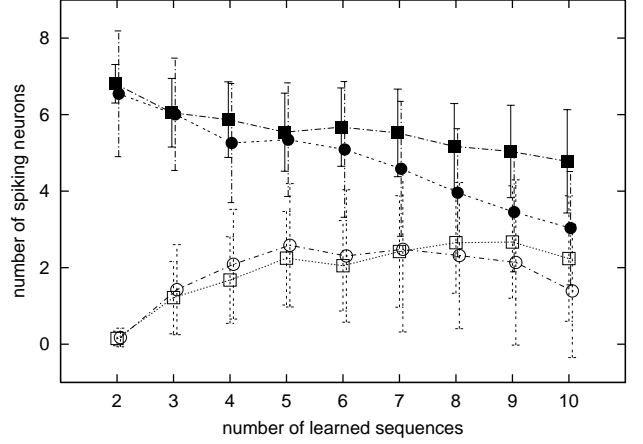


FIG. 10: Scaling storage quality with number of input sequences. A system with 50 neurons was trained with a varying number of input sequences of length 8. The figure shows the response after 16 s of training for each input sequence. The filled squares show the average number of responding neurons within a sequence and the open squares the number of responding neurons not in the sequence in response to input fractions of length 3 of the learned sequences. The filled circles and the open circles show the corresponding numbers in response to inputs of length 2. All data points are averages of 10 independent trials, i.e. 10 independent sets of input sequences.

put at the “input synapses”.

Fig. 11 shows the impact of noise on the learning performance. The upper left panel shows the effect of additive white noise at the membrane potential in the learning stage and the upper right panel the impact of this type of noise in both learning and recalling. As to be expected learning is far less sensitive to noise than the recalling due to the fact that the effect of the temporally uncorrelated noise on the synaptic strength is averaged out over time.

Unreliable input was implemented as random changes of the amplitude of the EPSPs exciting the HH neurons. The maximal conductance for each input synapse was chosen from a Gaussian distribution with mean 0.2 mS and standard deviations 0.05 mS , 0.1 mS , 0.15 mS , and 0.2 mS . The lower left panel of Fig. 11 shows the learning success if the unreliable input is applied during learning and the lower right panel if it is applied during learning and during recall. Again the recall is much more sensitive to the effects of the unreliability than the learning stage.

V. DISCUSSION

It has been demonstrated that synaptic plasticity allows the transformation of temporal information into spatial information providing an efficient mechanism for storing temporal sequences. The analysis and the numerical simulations show that the storage capacity of the

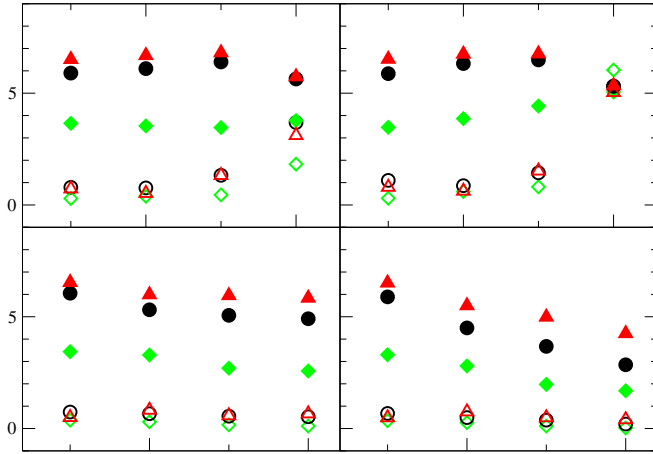


FIG. 11: Impact of different types of noise on the learning performance. Effects of additive white noise in the membrane potential applied during the learning state (upper left panel) and applied during learning and recall (upper right panel). The data points show the average response of the neurons within a test sequence to two inputs (filled diamonds), three inputs (filled circles) and four inputs (filled triangles). The average responses of neurons not belonging to the test sequence are shown for two (open diamonds), three (open circles) and four inputs (open triangles) as well. The values for the standard deviation of noise were 0.125 mV , 0.25 mV , 0.5 mV and 1.0 mV (x axes in the upper panels are on a logarithmic scale). The lower panels show the average response to two, three and four inputs of neurons in and out of the tested sequence if the strength of each input synapse is chosen according to Gaussian distribution with mean 0.2 mS and standard deviations 0.05 mS , 0.1 mS , 0.15 mS and 0.2 mS each time they are activated. In the lower left panel this unreliable input is only applied in the learning stage. In the lower right panel the input is unreliable in learning and recalling stage.

system is mainly limited by the statistical properties of the input, i.e. the overlap probabilities for randomly chosen input sequences. Having demonstrated the ability of a model system with biologically realistic model neurons to store temporal information using the experimentally based synaptic plasticity learning rule, we have taken an important step toward understanding the role of synaptic plasticity in the representation of time in biological systems.

The successful storage of arbitrary input sequences, however, crucially depends on the existence of the corresponding synapses making the all-to-all connections in the investigated system a necessary requirement. In re-

alistic systems such global all-to-all connections can not be found, but this might be compensated through divergence and redundancy of the input. If the density of connections and the number of neurons each input excites is high enough, pairs of connected neurons being excited by successive inputs will appear on a statistical basis. This mechanism will be discussed more thoroughly in forthcoming work.

The realistic implementation of saturation of synaptic strength for additive learning rules is another topic to be addressed in further work. For the system investigated here we implemented a combination of two mechanisms. On the one hand the synaptic strength was directly bounded by use of the sigmoid filtering function applied to the bare synaptic strength subject to the additive learning rule. On the other hand the steady decay of synaptic strength and the continuous stimulation of the network by the inputs lead to a dynamical steady state thereby bounding the synaptic strength dynamically.

Whereas the direct bound through a sigmoid filtering function might capture some aspects of the behavior of real synapses, the decay of synaptic strength necessary to achieve a realistic dynamical steady state is clearly too fast to be realistic. The system forgets much too fast if it is not continuously stimulated with appropriate input.

Alternative solutions to the saturation problem include competition based mechanisms suggested by recent findings of interactions of various kinds between neighboring synapses on a dendritic tree [37] and learning rules which depend on the synaptic strength itself like e.g. multiplicative learning rules.

The system is reasonably robust against noise. It is noteworthy that it is more sensitive to internal high-frequency noise than to noise in the incoming signals.

Acknowledgments

This work was partially supported by the U.S. Department of Energy, Office of Basic Energy Sciences, Division of Engineering and Geosciences, under Grants No. DE-FG03-90ER14138 and No. DE-FG03-96ER14592, by a grant from the National Science Foundation, NSF PHY0097134, by a grant from the Army Research Office, DAAD19-01-1-0026, by a grant from the Office of Naval Research, N00014-00-1-0181, and by a grant from the National Institutes of Health, NIH R01 NS40110-01A2.

[1] A. S. Dave, A. C. Yu, and D. Margoliash, *Science* **282**, 2250 (1998).
[2] A. C. Yu and D. Margoliash, *Science* **273**, 1871 (1996).
[3] R. v. Rullen and S. J. Thorpe, *Neural Comp.* **13**, 1255 (2001).
[4] G. Laurent, K. MacLeod, and M. Wehr, *Learn. & Mem.* **5**, 124 (1998).
[5] G. Laurent, *Science* **286**, 723 (1999).
[6] G. Laurent, M. Stopfer, R. W. Friedrich, M. I. Rabinovich, and H. D. I. Abarbanel, *Annu. Rev. Neurosci.* **24**, 263 (2001).
[7] P. Vetter, A. Roth, and M. Häusser, *J. Neurophysiol.* **85**,

926 (2001).

[8] M. Häusser, N. Spruston, and G. J. Stuart, *Science* **290**, 739 (2000).

[9] C. Koch, *Biophysics of computation: Information processing in single neurons* (Oxford University Press, New York, 1999).

[10] C. Koch, *Biol. Cybern.* **50**, 15 (1984).

[11] L. A. Jeffres, *J. Comp. Physiol. Psychol.* **41**, 35 (1948).

[12] A. Herz, B. Sulzer, R. Kühn, and J. L. van Hemmen, *Europhys. Lett.* **7**, 663 (1988).

[13] A. Herz, B. Sulzer, R. Kühn, and J. L. van Hemmen, *Biol. Cybern.* **60**, 457 (1989).

[14] C. Leibold, R. Kempter, and J. L. van Hemmen, *Phys. Rev. E* **65**, 051915 (2002).

[15] J. Rinzel, D. Terman, X. Wang, and B. Ermentrout, *Science* **279**, 1351 (1998).

[16] D. Colomb, X. J. Wang, and J. Rinzel, *J. Neurophysiol.* **75**, 750 (1996).

[17] J. E. Lisman and N. A. Otmakhova, *Hippocampus* **11**, 551 (2001).

[18] J. E. Lisman, *Neuron* **22**, 233 (1999).

[19] S. P. Tonkin and R. B. Pinter, *Network: Comput. Neural Syst.* **7**, 385 (1996).

[20] R. P. N. Rao and T. J. Sejnowski, in *Advances in Neural Information Processing Systems*, edited by S. A. Solla, T. K. Leen, and K.-R. Müller (2000), vol. 12, pp. 217–226.

[21] L. F. Abbott and K. I. Blum, *Cereb. Cortex* **6**, 406 (1996).

[22] M. R. Mehta, C. A. Barnes, and B. L. McNaughton, *Proc. Natl. Acad. Sci. USA* **94**, 8918 (1997).

[23] W. Gerstner and L. F. Abbott, *J. Comput. Neurosci.* **4**, 79 (1997).

[24] O. Jensen and J. E. Lisman, *Learn. & Mem.* **3**, 279 (1996).

[25] M. Rabinovich, A. Volkovskii, P. Lecanda, R. Huerta, H. D. I. Abarbanel, and G. Laurent, *Phys. Rev. Lett.* **87**, 068102 (2001).

[26] R. C. Malenka and R. A. Nicoll, *Science* **285**, 1870 (1999).

[27] D. J. Linden, *Neuron* **22**, 661 (1999).

[28] G. q. Bi and M. m. Poo, *Annu. Rev. Neurosci.* **24**, 139 (2001).

[29] S.-N. Yang, Y.-G. Tang, and R. S. Zucker, *J. Neurophysiol.* **81**, 781 (1999).

[30] H. Markram, J. Lübke, M. Frotscher, and B. Sakmann, *Science* **275**, 213 (1997).

[31] G. q. Bi and M. m. Poo, *J. Neurosci.* **18**, 10464 (1998).

[32] H. D. I. Abarbanel, R. Huerta, and M. I. Rabinovich, *Proc. Natl. Acad. Sci. USA* **99**, 10132 (2002).

[33] W. Rall, *J. Neurophys.* **30**, 1138 (1967).

[34] W. Rall, in *Methods in Neuronal Modeling: From synapses to networks*, edited by C. Koch and I. Segev (MIT Press, Cambridge, 1989), pp. 9–62.

[35] A. Destexhe, Z. F. Mainen, and T. J. Sejnowski, in *Methods in Neuronal Modeling, 2nd Ed.*, edited by C. Koch and I. Segev (MIT Press, Cambridge, MA, 1998), pp. 1–26.

[36] J. C. Butcher, *The Numerical Analysis of Ordinary Differential Equations* (Wiley, Chichester, 1987).

[37] N. Arnth-Jensen, D. Jabaudon, and M. Scanziani, *Nature Neuroscience* **5**, 325 (2002).